

Predictions for BAO distance estimates from the cross-correlation of the Lyman- α forest and redshifted 21-cm emission.

Tapomoy Guha Sarkar^a Somnath Bharadwaj^b

^aDepartment of Physics, Birla Institute of Technology and Science, Pilani, Rajasthan, India.

^bDepartment of Physics and Meteorology & Centre for Theoretical Studies, IIT, Kharagpur 721302, India.

E-mail: tapomoy@pilani.bits-pilani.ac.in, somnath@phy.iitkgp.ernet.in

Abstract.

We investigate the possibility of using the cross-correlation of the Lyman- α forest and redshifted 21-cm emission to detect the baryon acoustic oscillation (BAO). The standard Fisher matrix formalism is used to determine the accuracy with which it will be possible to measure cosmological distances using this signal. Earlier predictions [1] indicate that it will be possible to measure the dilation factor D_V with 1.9% accuracy at $z = 2.5$ from the BOSS Lyman- α forest auto-correlation. In this paper we investigate if it is possible to improve the accuracy using the cross-correlation.

We use a simple parametrization of the Lyman- α forest survey which very loosely matches some properties of the BOSS. For the redshifted 21-cm observations we consider a hypothetical radio interferometric array layout. It is assumed that the observations span $z = 2$ to 3 and covers the 10,000 deg² sky coverage of BOSS. We find that it is possible to significantly increase the accuracy of the distance estimates by considering the cross-correlation signal.

Contents

1	Introduction	1
2	The Cross-correlation Signal	3
3	The Cross-correlation Estimator	6
4	The Baryon Acoustic Oscillations	10
5	Observational Considerations	11
6	Results	13
6.1	Predictions for a BOSS-like survey	13
7	Acknowledgement	16

1 Introduction

Neutral hydrogen (HI) in the post-reionization epoch ($z < 6$) is known to be an important cosmological probe seen in both emission and absorption. Here, the redshifted 21-cm emission [2, 3] and the transmitted QSO flux through the Lyman- α forest [4, 5] are both of utmost observational interest. In a recent paper [6] have proposed the cross-correlation of the 21-cm signal with the Lyman- α forest as a new probe of the post-reionization era. While it is true that the emission and the absorption signals both originate from neutral hydrogen (HI) at the same redshift (or epoch), these two signals, however, do not originate from the same set of astrophysical sources. The 21-cm emission originates from the HI housed in the Damped Lyman- α systems (DLAs) which are known to contain the bulk of the HI at low redshifts [7]. The collective emission from the individual clouds appears as a diffuse background in low frequency radio observations [8]. On the contrary, the Lyman- α forest consists of a large number of Lyman- α absorption lines seen in the spectra of distant background quasars. These absorption features arises due to small density fluctuations in the predominantly ionized diffuse IGM. On large scales, however, the fluctuations in the 21-cm signal and the Lyman- α forest transmitted flux are both believed to be excellent tracers of the underlying dark matter distribution. It has been proposed [6] that the cross-correlation between these two signals can be used to probe the power spectrum during the post-reionization era.

The HI power spectrum can be determined separately from observations of the Lyman- α forest [9] and the redshifted 21-cm emission [10]. The cross-correlation signal, however, has some unique features which makes it interesting to also consider this as a probe of the HI power spectrum in addition to the respective auto-correlation signals. In order to highlight this, we first briefly discuss some aspects of the individual auto-correlation signals. First, it is only possible to detect the Lyman- α forest along discrete lines of sight to known

quasars. The Poisson noise arising from this discrete sampling is an important factor in limiting the accuracy to which the three dimensional auto-correlation power spectrum can be estimated from a given survey. This limit depends on the mean quasar number density and the signal to noise ratios (SNR) of the individual quasar spectra which varies from quasar to quasar [11]. Both of these are usually predetermined once the survey instrument and observational strategy are fixed, and it is typically not possible to improve these values further for a given survey. In contrast, the redshifted 21-cm signal is sensitive to the HI distribution in the entire field of view. The accuracy to which the auto-correlation power spectrum can be estimated is determined by the configuration of the radio-interferometric array and the system noise. It is, in principle, possible here to scale up the array and increase the observation time to reduce the system noise to a level where it is possible to measure the HI power spectrum at an accuracy that is comparable to the cosmic variance limit. The redshifted 21-cm signal, however, is buried in foregrounds from other astronomical sources like the galactic synchrotron emission, extra-galactic point sources, etc. Removing these foregrounds which are several orders of magnitude larger than the signal, poses a great challenge for detecting the post-reionization HI power spectrum [12, 13]. The foregrounds in the redshifted 21-cm emission will not be correlated with the Lyman- α forest. We therefore expect the foreground problem to be much less severe for the cross-correlation signal. In fact, any residual foreground after subtraction will only contribute to the variance of the cross-correlation signal. This is the key advantage of using the cross-correlation in comparison to the redshifted 21-cm auto-correlation. Comparing to the Lyman- α forest auto-correlation, the accuracy to which it is possible to estimate the cross-correlation power spectrum also is limited by the discrete QSO sampling. This dependence, however, is weaker for the cross-correlation as compared to the auto-correlation. Given a Lyman- α forest survey, it may be possible to suitably design redshifted 21-cm observations such that the cross-correlation provides a more accurate estimate of the power spectrum in comparison to the Lyman- α forest auto-correlation. These two features, namely less severe foreground problems compared to the 21-cm auto-correlation and the prospects of improving the SNR compared to the Lyman- α forest auto-correlation, provide motivation for considering the cross-correlation as a probe of the cosmological power spectrum.

Cosmological density perturbations drive acoustic waves in the primordial baryon-photon plasma which are frozen once recombination takes place at $z \sim 1000$, leaving a distinct oscillatory signature on the CMBR anisotropy power spectrum [14]. The sound horizon at recombination sets a standard ruler that maybe used to calibrate cosmological distances. Baryons contribute to 15% of the total matter density, and the baryon acoustic oscillations are imprinted in the late time clustering of non-relativistic matter. The signal, here, is however suppressed by a factor $\sim \Omega_b/\Omega_m \sim 0.1$, unlike the CMBR temperature anisotropies where it is an order unity effect [15]. The baryon acoustic oscillation (BAO) is a powerful probe of cosmological parameters [16, 17]. This is particularly useful since the effect occurs on large scales (~ 150 Mpc), where the fluctuations are still in the linear regime. It is possible to measure the an-

gular diameter distance $D_A(z)$ and the Hubble parameter $H(z)$ as functions of redshift using the the transverse and the longitudinal oscillations respectively. These provide means for estimating cosmological parameters and placing stringent constraints on dark energy models. Several groups have considered the possibility of detecting the BAO signal using redshift 21-cm emission [18–20]. Recently the BAO has been precisely measured at $z \sim 0.57$ [21] using the galaxies in the SDSS III Baryon Oscillation Spectroscopic Survey (BOSS; [1]). The possibility of detecting the BAO signal in the Lyman- α forest has been extensively studied [22]. The BAO has recently been detected at $z \sim 2.3$ [23, 24] using the BOSS Lyman- α forest data. The combination $D_A^{0.2} H^{-0.8}$ has been measured at a precision of 3.5%. The data used in these works covers about one-third of the ultimate BOSS footprint.

The projected results for BOSS [1] predict that at the end of the survey the overall dilation factor $D_A^{2/3} H^{-1/3}$ shall be measured from the Lyman- α data at an accuracy level of 1.9% at $z \sim 2.5$. In this paper we investigate the possibility of improving the accuracy of the distance estimates by measuring the cross-correlation of the BOSS Lyman- α data with redshifted 21-cm maps. We propose a possible radio-interferometric array configuration and discuss the observational strategy required to achieve this. The possibility of detecting the BAO using the cross-correlation signal has also been discussed in an earlier work [25] which investigates the possibility of detecting the BAO oscillatory feature in the cross-correlation multi-frequency angular power spectrum in the transverse and radial direction. The present work looks at the three dimensional cross power spectrum and makes predictions for the cosmological distance measures using a Fisher matrix analysis.

A brief outline of the paper follows. In Section 2 of this paper we quantify the cross-correlation between the Lyman- α forest and the 21-cm emission. In Section 3 we introduce an estimator for the cross-correlation signal and derive its statistical properties. In Section 4 we consider the imprint of BAO on the cross correlation signal and set up the Fisher matrix for theoretically estimating the accuracy to which it will be possible to measure $D_A(z)$ and $H(z)$. In section 5 we present several observational considerations and the strategy for measuring the cross-correlation signal. Finally, in Section 6 we present theoretical prediction of the accuracy at which it will be possible to measure D_A and $H(z)$. We have used a reference cosmological model with cosmological parameters $(\Omega_m h^2, \Omega_b h^2, \Omega_\Lambda, h, n_s, \sigma_8) = (0.136, 0.023, 0.726, 0.705, 0.97, 0.82)$ [15] throughout this paper.

2 The Cross-correlation Signal

We quantify the fluctuations in the transmitted flux $\mathcal{F}(\hat{n}, z)$ along a line of sight \hat{n} to a quasar through the Lyman- α forest using $\delta_{\mathcal{F}}(\hat{n}, z) = \mathcal{F}(\hat{n}, z)/\bar{\mathcal{F}} - 1$. For the purpose of this paper we are interested in large scales where it is reasonable to adopt the fluctuating Gunn-Peterson approximation [9, 26–28]. This relates the transmitted flux to the matter density contrast δ as $\mathcal{F} = \exp[-A(1 + \delta)^\kappa]$ which does not include redshift space distortion, and therefore gives only a rough picture. Here A and κ are two redshift dependent quantities. The function A

is of order unity [29] and depends on the mean flux level, IGM temperature, photo-ionization rate and cosmological parameters [28], while κ depends on the IGM temperature density relation [30, 31]. For our analytic treatment of the Lyman- α signal, we assume that the measured fluctuations $\delta_{\mathcal{F}}$ have been smoothed over a sufficiently large length scale such that it is adequate to work with only a linear term $\delta_{\mathcal{F}} \propto \delta$ [9, 27, 28, 32–34] which incorporates redshift space distortion and a possible bias (eq. 2.1). The terms of higher order in δ are expected to be important at small length scales which have not been considered here.

We use $\delta_T(\hat{n}, z)$ to quantify the fluctuations in $T(\hat{n}, z)$ the brightness temperature of redshifted 21-cm radiation. In the redshift range of our interest ($z < 3.5$), it is reasonable to assume that $\delta_T(\hat{n}, z)$ traces δ with a possible bias [8, 10]. The bias is expected to be scale dependent below the Jeans length-scale [35]. General non-linearity shall also make the bias scale dependent and further, fluctuations in the ionizing background also give rise to a scale dependent bias [36, 37]. This bias is moreover found to grow monotonically with z [38]. However, numerical simulations [39, 40], indicate that it is adequate to use a constant, scale independent bias at the large BAO scales of our interest.

With the above mentioned assumptions and incorporating redshift space distortions we may express both $\delta_{\mathcal{F}}$ and δ_T as

$$\delta_{\alpha}(\hat{n}, z) = \int \frac{d^3\mathbf{k}}{(2\pi)^3} e^{i\mathbf{k}\cdot\hat{n}r} C_{\alpha}[1 + \beta_{\alpha}\mu^2]\Delta(\mathbf{k}). \quad (2.1)$$

where $\alpha = \mathcal{F}$ and T refer to the Lyman- α forest and 21-cm signal respectively. Here r is the comoving distance corresponding to z , $\Delta(\mathbf{k})$ is the matter density contrast in Fourier space and $\mu = \hat{\mathbf{k}} \cdot \hat{\mathbf{n}}$. We adopt the values $C_{\mathcal{F}} = -0.13$ and $\beta_{\mathcal{F}} = 1.58$ from the Lyman- α forest simulations of [41] at $z = 2.25$. [42] have measured the 1-D power spectrum using the Lyman- α auto-correlation, and they present estimates of the redshift evolution of the bias in the z range 2 to 3. This bias, however, has a significant contribution from the statistical errors in the estimated mean flux $\bar{\mathcal{F}}$ which appears in the definition of $\delta_{\mathcal{F}}(\hat{n}, z)$. While this error causes a bias in the auto-correlation, we do not expect it to affect the cross-correlation considered here. To keep the analysis simple, we make the somewhat unrealistic assumption that bias for $\delta_{\mathcal{F}}(\hat{n}, z)$ is constant across the redshift range of our interest. While including this is important in the real data analysis, we do not expect this to severely affect the predictions of this paper. We use $C_T = \bar{T} \bar{x}_{\text{HI}} b$ and $\beta_T = f/b$ which can be calculated for any z for the 21-cm signal [6]. We note that there are large uncertainties in the values of all the four parameters $C_T, C_{\mathcal{F}}, \beta_T$ and $\beta_{\mathcal{F}}$ arising from our poor knowledge of the state of the diffuse IGM and the systems that harbour bulk of the neutral hydrogen at $z \sim 2.5$.

A QSO survey (eg. SDSS¹), typically, covers a large fraction of the entire sky. In contrast, a radio interferometric array (eg. GMRT²) usually has a much smaller field of view ($\sim 1^\circ$). Only the overlapping region common to both these

¹<http://www.sdss.org>

²<http://www.ncra.tifr.res.in>

observations provides an estimate of the cross-correlation signal. We therefore use the limited field of view $L \times L$ (L in radians) of the radio telescope to estimate the cross-correlation signal. Given this constraint, it is a reasonable observational strategy to use several pointings of the radio telescope to cover the entire region of the QSO survey. Each pointing of the radio telescope provides an independent estimate of the cross-correlation signal, which can be combined to reduce the cosmic variance.

We have assumed that the field of view is sufficiently small ($L \ll 1$) so that the curvature of the sky may be ignored. In the flat sky approximation, the unit vector \hat{n} along any line of sight can be expressed as $\hat{n} = \hat{\mathbf{m}} + \vec{\theta}$, where $\hat{\mathbf{m}}$ is the line of sight to the centre of the field of view and $\vec{\theta}$ is a two-dimensional ($2D$) vector on the plane of the sky. We further assume that the redshift range of the observation is restricted to a relatively narrow band B centered at the redshift z . We then have an $L \times L \times B$ observational volume, and we use the displacement $(\vec{\theta}, \Delta z)$ relative to the center as observational coordinates within this volume. We have the comoving displacement vector $\Delta \mathbf{r} = r\vec{\theta} + \Delta r \hat{\mathbf{m}}$ with $\Delta r = c\Delta z/H(z)$ corresponding to the observational coordinates $(\vec{\theta}, \Delta z)$.

It is convenient to decompose the observed $\delta_{\mathcal{F}}(\vec{\theta}, \Delta z)$ and $\delta_T(\vec{\theta}, \Delta z)$ into Fourier modes whereby

$$\Delta_{\alpha}(\mathbf{U}, \tau) = \int_{-B/2}^{B/2} d\Delta z \int_{-L/2}^{L/2} d^2\vec{\theta} e^{-2\pi i(\mathbf{U}\cdot\vec{\theta} + \tau \Delta z)} \delta_{\alpha}(\vec{\theta}, \Delta z) \quad (2.2)$$

where \mathbf{U} is a two dimensional vector conjugate to $\vec{\theta}$, and τ is conjugate to Δz .

We use the power spectra $\mathcal{P}_{\alpha\gamma}(U, \tau)$ to quantify the statistical properties of the observed fluctuation fields. These power spectra are defined through

$$\text{Re}\langle \Delta_{\alpha}(\mathbf{U}, \tau) \Delta_{\gamma}^*(\mathbf{U}', \tau') \rangle = L^2 B \delta_{\mathbf{U}\mathbf{U}'} \delta_{\tau\tau'} \mathcal{P}_{\alpha\gamma}(U, \tau), \quad (2.3)$$

and we have

$$\mathcal{P}_{\alpha\gamma}(U, \tau) = F_{\alpha\gamma}(\mu) P(k) \quad (2.4)$$

where $P(k)$ is the matter power spectrum and

$$F_{\alpha\gamma}(\mu) = \frac{H(z)}{r^2 c} C_{\alpha} C_{\gamma} (1 + \beta_{\alpha} \mu^2)(1 + \beta_{\gamma} \mu^2) \quad (2.5)$$

Here U refers to inverse angular scales and $\mathbf{k}_{\perp} = 2\pi\mathbf{U}/r$ refers to the component of the Fourier mode \mathbf{k} perpendicular to the line of sight, while τ refers to the inverse of Δz and $k_{\parallel} = 2\pi H(z)\tau/c$ refers to the line of sight component of the Fourier mode \mathbf{k} . In the subsequent analysis we use $\mathcal{P}_{\mathcal{FT}}(U, \tau)$ to quantify the statistical properties of the cross-correlation signal. We had earlier, in Paper I [6], used the multi-frequency angular power spectrum (MAPS, [43]) to quantify the cross-correlation signal. We note that the multi-frequency angular power spectrum $C_{\ell}(\Delta z)$ used earlier is the Fourier transform of the power spectrum $\mathcal{P}_{\mathcal{FT}}(U, \tau)$ that we use here *ie*.

$$C_{\ell}(\Delta z) = \int d\tau e^{2\pi i \Delta z \tau} \mathcal{P}_{\mathcal{FT}}(U, \tau). \quad (2.6)$$

with $\ell = 2\pi U$.

3 The Cross-correlation Estimator

In this section we construct an estimator for $P_{\mathcal{FT}}(U, \tau)$, and consider the statistical properties of this estimator. First, we assume that both the Lyman- α forest and the 21-cm observations are pixelized along the Δz axis into pixels or channels of width Δz_c such that both $\delta_{\mathcal{F}}(\vec{\theta}, \Delta z)$ and $\delta_T(\vec{\theta}, \Delta z)$ are measured only at discrete redshifts $\Delta z_n = n\Delta z_c$ with $n = -N_c/2 + 1, \dots, -2, -1, 0, 1, 2, \dots, N_c/2$. Here $N_c + 1$ is the total number of channels, and $(N_c + 1)\Delta z_c = B$ is the total redshift interval or the bandwidth spanned by the observations.

Considering first the Lyman- α forest, we have, till now, considered $\delta_{\mathcal{F}}(\vec{\theta}, \Delta z_n)$ as a continuous field defined at all points on the sky. In reality, it is possible to measure this only along a few, discrete lines of sight where there are background quasars. We account for this by defining $\delta_{\mathcal{F}_o}(\vec{\theta}, n)$, the observed fluctuation in the transmitted Lyman- α flux, as

$$\delta_{\mathcal{F}_o}(\vec{\theta}, n) = \rho(\vec{\theta}) [\delta_{\mathcal{F}}(\vec{\theta}, \Delta z_n) + \delta_{\mathcal{FN}}(\vec{\theta}, n)] \quad (3.1)$$

where $\delta_{\mathcal{FN}}(\vec{\theta}, n)$ is the contribution from the pixel noise in the quasar spectra and

$$\rho(\vec{\theta}) = \frac{\sum_a w_a \delta_D^2(\vec{\theta} - \vec{\theta}_a)}{\sum_a w_a} \quad (3.2)$$

is the quasar sampling function. Here $a = 1, 2, \dots, N$ refers to the different quasars in the $L \times L$ field of view, $\vec{\theta}_a$ and w_a respectively refer to the angular positions and weights of the individual quasars. We have the freedom of adjusting the weights to suit our convenience. It is possible to change the relative contribution from the individual quasars by adjusting the weights w_a .

The quasar sampling function $\rho(\vec{\theta})$ is zero everywhere except the angular position of the different quasars. It is sometimes convenient to express the noise contribution in eq. (3.1) as

$$\rho(\vec{\theta}) \delta_{\mathcal{FN}}(\vec{\theta}, n) = \frac{\sum_a w_a \delta_D^2(\vec{\theta} - \vec{\theta}_a) \delta_{\mathcal{FN}}(\vec{\theta}_a, n)}{\sum_a w_a} \quad (3.3)$$

where $\delta_{\mathcal{FN}}(\vec{\theta}_a, n)$ refers to the pixel noise contribution for the different quasars. The faint quasars typically have noisy spectra in comparison to the bright ones. We can take this into account and choose the weights w_a so as to increase the contribution from the bright quasars relative to the faint ones, thereby maximizing the SNR for the signal estimator. For the present analysis we have made the simplifying assumption that the magnitude of $\delta_{\mathcal{FN}}(\vec{\theta}_a, n)$ is the same across all the quasars irrespective of the quasar flux. We have modelled $\delta_{\mathcal{FN}}(\vec{\theta}_a, n)$ as Gaussian random variables with the noise in the different pixels being uncorrelated *ie.*

$$\langle \delta_{\mathcal{FN}}(\vec{\theta}_a, n) \delta_{\mathcal{FN}}(\vec{\theta}_b, m) \rangle = \delta_{a,b} \delta_{n,m} \sigma_{\mathcal{FN}}^2 \quad (3.4)$$

where $\sigma_{\mathcal{FN}}^2$ is the variance of the pixel noise contribution. It is appropriate to use uniform weights $w_a = 1$ in this situation. Such an assumption is justified

in the situation where there exist high SNR measurements of the transmitted flux for all the quasars.

Considering next the sampling function $\rho(\vec{\theta})$, we assume that the quasars are randomly distributed with no correlation amongst their angular position, and the positions also being unrelated to $\delta_{\mathcal{F}}$ and δ_T . In reality, the quasars do exhibit clustering [44], however the contribution from the Poisson fluctuation is considerably more significant here and it is quite justified to ignore the effect of quasar clustering for the present purpose. The Fourier transform of $\rho(\vec{\theta})$ then has the properties that

$$\langle \tilde{\rho}(\mathbf{U}) \rangle = \delta_{\mathbf{U},0} \quad (3.5)$$

and

$$\langle \tilde{\rho}(\mathbf{U}_1) \tilde{\rho}(\mathbf{U}_2) \rangle = \frac{1}{N} \delta_{\mathbf{U}_1, \mathbf{U}_2} + \left(1 - \frac{1}{N}\right) \delta_{\mathbf{U}_1, 0} \delta_{\mathbf{U}_2, 0} \quad (3.6)$$

which we shall use later. In the subsequent analysis, we also assume that $N \gg 1$ whereby $(1 - 1/N) \approx 1$.

We use $\Delta_{\mathcal{F}o}(\mathbf{U}, \tau)$ to denote the Fourier transform of $\delta_{\mathcal{F}o}(\vec{\theta}, \Delta z)$. Using eq. (3.1) we have

$$\Delta_{\mathcal{F}o}(\mathbf{U}, \tau) = \tilde{\rho}(\mathbf{U}) \otimes [\Delta_{\mathcal{F}}(\mathbf{U}, \tau) + \Delta_{\mathcal{F}N}(\mathbf{U}, \tau)] \quad (3.7)$$

where \otimes denotes a convolution defined as

$$\tilde{\rho}(\mathbf{U}) \otimes \Delta_{\mathcal{F}}(\mathbf{U}, \tau) = \frac{1}{L^2} \sum_{\vec{U}'} \tilde{\rho}(\mathbf{U} - \vec{U}') \Delta_{\mathcal{F}}(\vec{U}', \tau) \quad (3.8)$$

Using eqs. (2.4), (3.3), (3.4), (3.5), (3.6) and (3.7) we calculate the following statistical properties of $\Delta_{\mathcal{F}o}$,

$$\langle \Delta_{\mathcal{F}o}(\mathbf{U}, \tau) \rangle = 0 \quad (3.9)$$

and

$$\begin{aligned} \langle \Delta_{\mathcal{F}o}(\mathbf{U}_1, \tau_1) \Delta_{\mathcal{F}o}^*(\mathbf{U}_2, \tau_2) \rangle &= \delta_{\mathbf{U}_1, \mathbf{U}_2} \delta_{\tau_1, \tau_2} \frac{B}{L^2} [\mathcal{P}_{\mathcal{F}\mathcal{F}}(\mathbf{U}_1, \tau_1) \\ &+ \frac{1}{n_Q} \left\{ L^{-2} \sum_{\mathbf{U}} \mathcal{P}_{\mathcal{F}\mathcal{F}}(\mathbf{U}, \tau_1) + \Delta z_c \sigma_{\mathcal{F}N}^2 \right\}] \end{aligned} \quad (3.10)$$

where $\bar{n}_Q = N/L^2$ denotes the quasar density on the sky.

It is possible to simplify the sum over \mathbf{U} using Parseval's theorem whereby

$$\frac{1}{L^2} \sum_{\mathbf{U}} \mathcal{P}_{\mathcal{F}\mathcal{F}}(\mathbf{U}, \tau) = p_{1D}(\tau) \quad (3.11)$$

and

$$p_{1D}(\tau) = \int d\Delta z e^{2\pi i \tau \Delta z} \xi_{\mathcal{F}}(\Delta z). \quad (3.12)$$

Here $\xi_{\mathcal{F}}(\Delta z) = \langle \delta_{\mathcal{F}}(\vec{\theta}_a, z_1) \delta_{\mathcal{F}}(\vec{\theta}_a, z_1 + \Delta z) \rangle$ is the one dimensional (1D) correlation function of the fluctuations in the transmitted flux along individual quasar

spectra, and $p_{1D}(\tau)$ is the 1D power spectrum corresponding to $\xi_{\mathcal{F}}(\Delta z)$. The 1D correlation $\xi_{\mathcal{F}}(\Delta z)$, or equivalently $\xi_{\mathcal{F}}(v_{\parallel})$, is traditionally used to quantify the Lyman- α forest along quasar spectra, and this has been quite extensively studied [45–47].

We have

$$\langle \Delta_{\mathcal{F}o}(\mathbf{U}_1, \tau_1) \Delta_{\mathcal{F}o}^*(\mathbf{U}_2, \tau_2) \rangle = \delta_{\mathbf{U}_1, \mathbf{U}_2} \delta_{\tau_1, \tau_2} L^{-2} B \mathcal{P}_{\mathcal{F}o}(\mathbf{U}_1, \tau_1) \quad (3.13)$$

where

$$\mathcal{P}_{\mathcal{F}o}(\mathbf{U}, \tau) = \mathcal{P}_{\mathcal{F}\mathcal{F}}(U, \tau) + \frac{1}{\bar{n}_Q} [p_{1D}(\tau) + \Delta z_c \sigma_{\mathcal{F}N}^2] \quad (3.14)$$

Here the term $\frac{1}{\bar{n}_Q} [p_{1D}(\tau) + \Delta z_c \sigma_{\mathcal{F}N}^2]$ arises due to the discrete quasar sampling. We note that in our work the quasar density \bar{n}_Q has been assumed to be constant over the redshift range of interest. In reality n_Q will exhibit a redshift dependence depending on the quasar luminosity function and the magnitude limit of the quasar survey [48], and it is necessary to take this into account.

Radio interferometric observations directly measure $\Delta_{T_o}(\mathbf{U}, \Delta z_n)$ which are related to $\Delta_{T_o}(\mathbf{U}, \tau)$ through a Fourier transform

$$\Delta_{T_o}(\mathbf{U}, \tau) = \int d\Delta z e^{-2\pi i \Delta z \tau} \Delta_{T_o}(\mathbf{U}, \Delta z). \quad (3.15)$$

We consider a radio-interferometric array with several antennas, each of diameter D . The antenna diameter and the field of view L are related as $\lambda/D \approx L$, where λ is the observing wavelength. Each pair of antennas measures $\Delta_T(\mathbf{U}, z_n)$ at a particular \mathbf{U} mode corresponding to $\mathbf{U} = \mathbf{d}/\lambda$, where \mathbf{d} is the antenna separation projected perpendicular to the line of sight. The baselines \mathbf{U} corresponding to the different antenna pairs are, in general, arbitrarily distributed depending on the array configuration. The observed HI fluctuation $\Delta_{T_o}(\mathbf{U}, n)$ at two different \mathbf{U} values are correlated if $|\mathbf{U}_1 - \mathbf{U}_2| \leq 1/L$. It is possible to combine the baselines where the signal is correlated by binning the \mathbf{U} values using cells of size $L^{-1} \times L^{-1}$. We then have the binned baselines at $\mathbf{U} = (n_x \hat{i} + n_y \hat{j})/L$ (n_x, n_y are integers) which exactly match the Fourier modes of the Lyman- α signal. The HI signal at different \mathbf{U} values are now uncorrelated.

We first considering only $\Delta_{TN}(\mathbf{U}, \Delta z_n)$ which is the noise contribution to $\Delta_{T_o}(\mathbf{U}, \Delta z_n)$. The noise in different channels and baselines is uncorrelated, and we have

$$\langle \Delta_{TN}(\mathbf{U}_1, \Delta z_n) \Delta_{TN}^*(\mathbf{U}_2, \Delta z_m) \rangle = \delta_{\mathbf{U}_1, \mathbf{U}_2} \delta_{n,m} L^2 N_T(\mathbf{U}_1) \quad (3.16)$$

Here $N_T(\mathbf{U})$ is the noise power spectrum. For a single polarization and a single baseline, this is given by

$$N_T(\mathbf{U}) = \left(\frac{T_{\text{sys}}^2}{2 \Delta \nu_c \Delta t} \right) \frac{[\int d\Omega \mathcal{P}(\vec{\theta})]^2}{[\int d\Omega \mathcal{P}^2(\vec{\theta})]} \quad (3.17)$$

where T_{sys} is the system temperature, $\Delta \nu_c$ the frequency interval corresponding to Δz_c , Δt the integration time and $\mathcal{P}(\vec{\theta})$ is the normalised power pattern of

the individual antennas [49]. The exact value of the ratio of the two integrals in eq. (3.17) depend on the antenna design. It is convenient here to express eq. (3.17) as

$$N_T(\mathbf{U}) = \frac{T_{\text{sys}}^2 L^2}{\chi N_{\text{pol}} M(\mathbf{U}) \Delta\nu_c \Delta t}. \quad (3.18)$$

where N_{pol} is the number of polarizations being used, $M(\mathbf{U})$ the number of baselines in the particular cell corresponding to \mathbf{U} , and χ is a factor whose value depends on the antenna beam pattern $\mathcal{P}(\vec{\theta})$. For the purpose of this paper it is reasonable to assume a value $\chi = 0.5$.

Writing

$$\Delta_{T_o}(\mathbf{U}, \tau) = \Delta_T(\mathbf{U}, \tau) + \Delta_{T_N}(\mathbf{U}, \tau) \quad (3.19)$$

we have

$$\langle \Delta_{T_N}(\mathbf{U}_1, \tau_1) \Delta_{T_N}^*(\mathbf{U}_2, \tau_2) \rangle = \delta_{\mathbf{U}_1, \mathbf{U}_2} \delta_{\tau_1, \tau_2} L^2 B \mathcal{P}_{T_o}(\mathbf{U}_1, \tau_1) \quad (3.20)$$

where

$$\mathcal{P}_{T_o}(\mathbf{U}, \tau) = \mathcal{P}_{TT}(U, \tau) + \Delta z_c N_T(\mathbf{U}). \quad (3.21)$$

We finally consider the cross-correlation for which we have

$$\text{Re} \langle \frac{1}{2} [\Delta_{\mathcal{F}_o}(\mathbf{U}_1, \tau_1) \Delta_{T_o}^*(\mathbf{U}_2, \tau_2) + \Delta_{\mathcal{F}_o}^*(\mathbf{U}_1, \tau_1) \Delta_{T_o}(\mathbf{U}_2, \tau_2)] \rangle = \delta_{\mathbf{U}_1, \mathbf{U}_2} \delta_{\tau_1, \tau_2} B \mathcal{P}_{\mathcal{F}_o}(\mathbf{U}_1, \tau_1) \quad (3.22)$$

where

$$\mathcal{P}_{\mathcal{F}_o}(\mathbf{U}, \tau) = \mathcal{P}_{\mathcal{F}_T}(U, \tau). \quad (3.23)$$

We use this to define the estimator $\hat{E}(\mathbf{U}, \tau)$ as

$$E(U, \tau) = \frac{1}{2B} [\Delta_{\mathcal{F}_o}(\mathbf{U}, \tau) \Delta_{T_o}^*(\mathbf{U}, \tau) + \Delta_{\mathcal{F}_o}^*(\mathbf{U}, \tau) \Delta_{T_o}(\mathbf{U}, \tau)] \quad (3.24)$$

The estimator has the property that

$$\langle E(\mathbf{U}, p) \rangle = \mathcal{P}_{\mathcal{F}_T}(U, \tau) \quad (3.25)$$

ie. it is an unbiased estimator for the cross-correlation signal. We next consider the covariance of the estimator

$$\text{cov}[E(\mathbf{U}_1, \tau_1), E(\mathbf{U}_2, \tau_2)] = \langle E(\mathbf{U}_1, \tau_1) E(\mathbf{U}_2, \tau_2) \rangle - \langle E(\mathbf{U}_1, \tau_1) \rangle \langle E(\mathbf{U}_2, \tau_2) \rangle \quad (3.26)$$

which, we find, is diagonal

$$\text{cov}[E(\mathbf{U}_1, \tau_1), E(\mathbf{U}_2, \tau_2)] = \delta_{\mathbf{U}_1, \mathbf{U}_2} \delta_{\tau_1, \tau_2} \sigma^2[E(\mathbf{U}_1, \tau_1)] \quad (3.27)$$

and we need only consider the variance

$$\sigma^2[E(\mathbf{U}, \tau)] = \langle E^2(\mathbf{U}, \tau) \rangle - \langle E(\mathbf{U}, \tau) \rangle^2 \quad (3.28)$$

which has a value

$$\Delta \mathcal{P}_{\mathcal{F}_T}^2(\mathbf{U}, \tau) \equiv \sigma^2[E(\mathbf{U}, \tau)] = \frac{1}{2} [\mathcal{P}_{\mathcal{F}_T}^2(U, \tau) + \mathcal{P}_{\mathcal{F}_o}(\mathbf{U}, \tau) \mathcal{P}_{T_o}(\mathbf{U}, \tau)] \quad (3.29)$$

We use eq. (3.29) along with eqs. (3.14) and (3.21) to calculate the error in the estimated cross-correlation power spectrum.

4 The Baryon Acoustic Oscillations

The characteristic scale of the BAO is set by the sound horizon s at the epoch of recombination given by

$$s = \int_a^{a_r} \frac{c_s(a)}{a^2 H(a)} da \quad (4.1)$$

where a_r is the scale factor at the epoch of recombination and c_s is the sound speed given by $c_s(a) = c/\sqrt{3(1 + 3\rho_b/4\rho_\gamma)}$, where ρ_b and ρ_γ denotes the photon and baryonic densities respectively. The comoving length-scale s defines a transverse angular scale $\theta_s = s[(1+z)D_A(z)]^{-1}$ and a radial redshift interval $\Delta z_s = sH(z)/c$, where $D_A(z)$ and $H(z)$ are the angular diameter distance and Hubble parameter respectively. The comoving length-scale $s = 143$ Mpc corresponds to $\theta_s = 1.38^\circ$ and $\Delta z_s = 0.07$ at $z = 2.5$. Measurement of θ_s and Δz_s separately, allows the independent determination of $D_A(z)$ and $H(z)$. Here we consider the determination of these two parameters from the BAO imprint on the cross-correlation signal. We now derive formulas to make error predictions for these parameters.

We start with the Fisher matrix

$$F_{ij} = \sum_{\mathbf{U}} \sum_{\tau} \frac{1}{\Delta \mathcal{P}_{\mathcal{F}T}^2(\mathbf{U}, \tau)} \frac{\partial \mathcal{P}_{\mathcal{F}T}(\mathbf{U}, \tau)}{\partial q_i} \frac{\partial \mathcal{P}_{\mathcal{F}T}(\mathbf{U}, \tau)}{\partial q_j} \quad (4.2)$$

where q_i refer to the cosmological parameters to be constrained.

it is convenient to approximate the sums by integrals using

$$\sum_{\mathbf{U}} \sum_{\tau} = \frac{1}{2} \int \frac{d^2 \mathbf{U}}{L^{-2}} \int \frac{d\tau}{B^{-1}} = \frac{V}{2(2\pi)^3} \int d\mathbf{k}_\perp \int dk_\parallel \quad (4.3)$$

where L^{-2} and B^{-1} are the cell sizes for \mathbf{U} and τ respectively, the factor 1/2 is included to account for the fact that (\mathbf{U}, τ) and $(-\mathbf{U}, -\tau)$ do not contain independent information and $V = r^2 L^2 B c / H(z)$ is the observational volume. The integrals have limits defined by $|\mathbf{U}| \leq U_{max}$ and $-(2\Delta z_c)^{-1} \leq \tau \leq (2\Delta z_c)^{-1}$, or equivalently $|\mathbf{k}_\perp| \leq 2\pi U_{max}/r$ and $-c(2\Delta z_c H(z))^{-1} \leq k_\parallel \leq c(2\Delta z_c H(z))^{-1}$ where U_{max} is the largest baseline in the radio interferometric array. We then have the Fisher matrix

$$F_{ij} = \frac{V}{(2\pi)^3} \int \frac{d^3 \mathbf{k}}{[\mathcal{P}_{\mathcal{F}T}^2(\mathbf{k}) + \mathcal{P}_{\mathcal{F}Fo}(\mathbf{k})\mathcal{P}_{TTo}(\mathbf{k})]} \frac{\partial \mathcal{P}_{\mathcal{F}T}(\mathbf{k})}{\partial q_i} \frac{\partial \mathcal{P}_{\mathcal{F}T}(\mathbf{k})}{\partial q_j} \quad (4.4)$$

which contains cosmological information from a variety of sources including the redshift space distortion and the Alcock-Paczynski effect. In this work we would like to isolate the BAO constraints and ignore everything else. This BAO information is mainly present at small wave numbers with the first peak at roughly $k \sim 0.045 \text{Mpc}^{-1}$. The subsequent wiggles are well suppressed by $k \sim 0.3 \text{Mpc}^{-1}$ which is within the limits of the \mathbf{k}_\perp and k_\parallel integrals. It is thus quite justified to ignore the limits of the integral in eq. (4.4) and treat it as

an integral over the entire \mathbf{k} space. Further, the BAO information is entirely contained in $P(k)$ and not $F_{\alpha\gamma}(\mu)$. We then have

$$F_{ij} = \frac{V}{(2\pi)^2} \int k^2 dk \int_{-1}^1 d\mu \frac{1}{[P^2(k) + \mathcal{P}_{\mathcal{F}\mathcal{F}o}(\mathbf{k})\mathcal{P}_{TTo}(\mathbf{k})/F_{\mathcal{F}T}^2(\mu)]} \frac{\partial P(\mathbf{k})}{\partial q_i} \frac{\partial P(\mathbf{k})}{\partial q_j} \quad (4.5)$$

The subsequent analysis closely follows [50], and we refer the reader there for more details. We use $P_b = P - P_c$ to isolate the baryonic features in the power spectrum, and we use this in the derivative $\partial P(k)/\partial q_i$. Here P_c refers to the CDM power spectrum without any baryonic features. This gives

$$P_b(\mathbf{k}) = \sqrt{8\pi^2} A \frac{\sin x}{x} \exp \left[- \left(\frac{k}{k_{silk}} \right)^{1.4} \right] \exp \left[- \left(\frac{k^2}{2k_{nl}^2} \right) \right] \quad (4.6)$$

where k_{silk} and k_{nl} denotes the scale of ‘Silk-damping’ and ‘non-linearity’ respectively. In our analysis we have used $k_{nl} = (3.07 h^{-1} \text{Mpc})^{-1}$ and $k_{silk} = (7.76 h^{-1} \text{Mpc})^{-1}$ from [50]. Here A is a normalization constant and $x = \sqrt{k_{\perp}^2 s_{\perp}^2 + k_{\parallel}^2 s_{\parallel}^2}$ where s_{\perp} and s_{\parallel} corresponds to θ_s and Δz_s in units of distance. The value of s is known to a high level of precision from CMBR observations, and the values of s_{\perp} and s_{\parallel} are equal to s for the reference values of D_A and $H(z)$. Changes in D_A and $H(z)$ are reflected as changes in the values of s_{\perp} and s_{\parallel} respectively, and the fractional errors in s_{\perp} and s_{\parallel} correspond to fractional errors in D_A and $H(z)$ respectively. We use $q_1 = \ln(s_{\perp}^{-1})$ and $q_2 = \ln(s_{\parallel})$ as parameters in our analysis, and determine the precision at which it will be possible to constrain these using the location of the BAO features in the cross-correlation signal. Following [50] we have the 2 – D Fisher matrix

$$F_{ij} = V A^2 \int dk \int_{-1}^1 d\mu \frac{k^2 \exp[-2(k/k_{silk})^{1.4} - (k/k_{nl})^2]}{[P^2(k) + \mathcal{P}_{\mathcal{F}\mathcal{F}o}(\mathbf{k})\mathcal{P}_{TTo}(\mathbf{k})/F_{\mathcal{F}T}^2(\mu)]} f_i(\mu) f_j(\mu) \quad (4.7)$$

where $f_1 = \mu^2 - 1$ and $f_2 = \mu^2$. We use the Cramer-Rao bound $\delta q_i = \sqrt{F_{ii}^{-1}}$ to calculate the error in the parameter q_i . A combined distance measure D_V , also referred to as the ‘dilation factor’ [51]

$$D_V(z)^3 = (1+z)^2 D_A(z) \frac{cz}{H(z)} \quad (4.8)$$

is often used as a single parameter to quantify BAO observations. We use $\delta D_V/D_V = \frac{1}{3}(4F_{11}^{-1} + 4F_{12}^{-1} + F_{22}^{-1})^{0.5}$ to calculate the relative error in D_V . The dilation factor is particularly useful when the sensitivity of the individual measurements of D_A and $H(z)$ is low.

5 Observational Considerations

The quasar redshift distribution peaks in the range $z = 2$ to 3 [52], and for our analysis we only consider the quasars in this redshift range. For a quasar at a redshift z_Q , the region $10,000 \text{ km s}^{-1}$ blue-wards of the quasar’s Lyman- α

emission is excluded from the Lyman- α forest due to the quasar's proximity effect. Further, only the pixels at least $1,000 \text{ km s}^{-1}$ red-ward of the quasar's Lyman- β and O-VI lines are considered to avoid the possibility of confusing the Lyman- α forest with the Lyman- β forest or the intrinsic O-VI absorption. For a quasar at the fiducial redshift $z_Q = 2.5$, the above considerations would allow the Lyman- α forest to be measured in the redshift range $1.96 \leq z \leq 2.39$ spanning an interval $\Delta z = 0.43$.

We consider redshifted 21 cm observations of bandwidth 128MHz covering the frequency range 355 MHz to 483MHz which corresponds to the redshift range $1.94 \leq z \leq 3$. The Lyman- α forest of any particular quasar will be measured in a smaller interval $\Delta z \approx 0.4$ which is the deciding factor for the cross-correlation signal. Thus, only a fraction (approximately 40%) of the total number of quasars in this redshift range 2 to 3 will contribute to the cross-correlation signal at any redshift z . We incorporate this in our estimates by noting that \bar{n}_Q in eq. (3.14) refers to only 40% of all the quasars in the entire z range 2 to 3.

We now discuss the kind of radio-interferometer that will be required. The response of a radio-interferometric array falls at angular scales that are comparable to the field of view of the individual antenna elements in the array, and it is not sensitive to angular scales that are larger than this field of view. The BAO scale subtends an angle of 1.56° at $z = 2.0$ and smaller angles at higher redshifts. In our analysis we consider a radio-interferometric array which has antennas elements that are $2 \text{ m} \times 2 \text{ m}$ in dimension. The array has a $L = 20^\circ$ field of view which is considerably larger than the BAO angular scale.

We next discuss the array layout that would be required to observe the BAO features. In particular, we would like to determine the antenna spacings that are required for the array to be sensitive to the BAO features. The first BAO peak is at roughly $k_a \sim 0.045 \text{ Mpc}^{-1}$, followed by subsequent wiggles whose amplitude is well suppressed within $k_b \sim 0.3 \text{ Mpc}^{-1}$. Using $d/\lambda = U = k r/2\pi$, we estimate that the Fourier modes k_a and k_b correspond to antenna separations $d_a = 31 \text{ m}$ and $d_b = 207 \text{ m}$ respectively. These figures roughly indicate the range of antenna spacings that would be required in the radio-interferometric array. Based on these considerations we consider a radio interferometric array which has N_{ann} antennas distributed such that all the baselines \vec{d} within $d_{max} = 250 \text{ m}$ are uniformly sampled, whereby $M(\mathbf{U})$ is independent of \mathbf{U} and we have $M(\mathbf{U}) \approx (N_{ann}/250)^2$. Using this in eq. (3.18), assuming $T_{sys} = 100 \text{ K}$, $N_{pol} = 2$, $\chi = 0.5$ we have

$$N_T = 1.0 \times 10^{-3} [\text{mK}]^2 \left(\frac{500}{N_{ann}} \right)^2 \left(\frac{100 \text{ KHz}}{\Delta \nu_c} \right) \left(\frac{1000 \text{ hrs}}{\Delta t} \right). \quad (5.1)$$

We have $k_{max} = 0.36 \text{ Mpc}^{-1}$ corresponding to $d_{max} = 250 \text{ m}$. The BAO features are well suppressed within k_{max} , and this is large enough to capture the entire BAO information.

The recent analysis of the BOSS Lyman- α forest auto-correlation [23] has used pixels of width 210 km s^{-1} for which they find a mean pixel SNR of 5.17. In our analysis we have assumed that the Lyman- α forest and the redshifted 21-cm

data are both smoothed to this pixel size which corresponds to $\Delta z_c = 2.45 \times 10^{-3}$ and $\Delta \nu_c = 284$ kHz, or equivalently a radial separation of $2 h^{-1}$ Mpc at $z = 2.5$. We also assume that all the pixels have the same SNR of 5.17. Finally we note that the noise term in $\mathcal{P}_{\mathcal{F}\mathcal{F}o}$ also depends on $\xi_{\mathcal{F}}$ for which we have used the values from [45].

6 Results

We present the results combining the entire redshift range into a single bin centered at $z = 2.5$. We have considered a total sky coverage of $\sim 10,000 \text{deg}^2$, which approximately matches the ultimate sky coverage of BOSS and which corresponds to 25 pointings of the $20^\circ \times 20^\circ$ field of view of the radio interferometer considered here. The value of the BAO length scale s is well constrained from CMBR observations. We have used the values $s_{\perp} = s_{\parallel} = 1$ (in units of the BAO length scale $s = 143 \text{Mpc}$) for the reference cosmological model. We use the Fisher matrix (eq. 4.7) to predict the uncertainty in the parameters $q_1 = \ln(s_{\perp}^{-1})$ and $q_2 = \ln(s_{\parallel})$, where $\delta D_A/D_A = |\delta q_1|$ and $\delta H/H = |\delta q_2|$.

For the observational framework outlined in Section 5, the Fisher matrix essentially depends on the two observational parameters \bar{n}_Q and N_T . To recapitulate, \bar{n}_Q refers to approximately 0.4 times the total angular density of quasars in the redshift range 2 to 3, and N_T is the system noise which depends on the number of antennas N_{ann} and the observing time Δt (eq. 5.1). The limits $\bar{n}_Q \rightarrow \infty$ and $N_T \rightarrow 0$, which correspond to $\mathcal{P}_{\mathcal{F}\mathcal{F}o} \rightarrow \mathcal{P}_{\mathcal{F}\mathcal{F}}$ (eq. 3.14) and $\mathcal{P}_{TTo} \rightarrow \mathcal{P}_{TT}$ (eq. 3.21) respectively, set the upper bound for the SNR, which also corresponds to the cosmic variance. In this limit, where the SNR depends only on the volume corresponding to the total field of view and the $B = 1.0$ redshift interval, we have $\delta D_V/D_V = 0.15\%$, $\delta H/H = 0.25\%$ and $D_A/D_A = 0.15\%$ which are independent of any of the other observational details. Figure 1 shows contours of $\delta D_V/D_V$ as a function of \bar{n}_Q and N_T . The fractional errors decrease very slowly beyond $\bar{n}_Q > 50 \text{deg}^{-2}$ or $N_T < 10^{-6} \text{mK}^2$ at the bottom right corner of the panels, and the cosmic variance limit is reached beyond the range shown in the figure.

The parameter values $\bar{n}_Q \sim 6 \text{deg}^{-2}$ and $N_T \sim 4.7 \times 10^{-5} \text{mK}^2$, we see, are adequate for a 1% accuracy, whereas $\bar{n}_Q \sim 2 \text{deg}^{-2}$ and $N_T \sim 3 \times 10^{-3} \text{mK}^2$ are adequate for a $\sim 10\%$ accuracy in D_V . The $\delta D_A/D_A$ and $\delta H/H$ contours which are not shown here exhibit a \bar{n}_Q and N_T dependence which is very similar to $\delta D_V/D_V$. Typically, it is possible to measure D_V at a higher level of precision compared to D_A and H for the same set of observational parameters.

6.1 Predictions for a BOSS-like survey

The ongoing BOSS [1, 52] has a quasar number density of $\approx 16 \text{deg}^{-2}$ implying $\bar{n}_Q = 6.4 \text{deg}^{-2}$ and is expected to cover $\sim 10,000 \text{deg}^2$ of the sky. It has been predicted that it will be possible to measure the dilation factor with an accuracy of $\delta D_V/D_V = 1.9\%$ at $z = 2.5$ from the Lyman- α forest auto-correlation using BOSS [1]. We now consider the cross-correlation signal for a BOSS-like survey. We investigate if it will be possible to improve the accuracy of the distance estimates by using the cross-correlation with redshifted 21-cm observations.

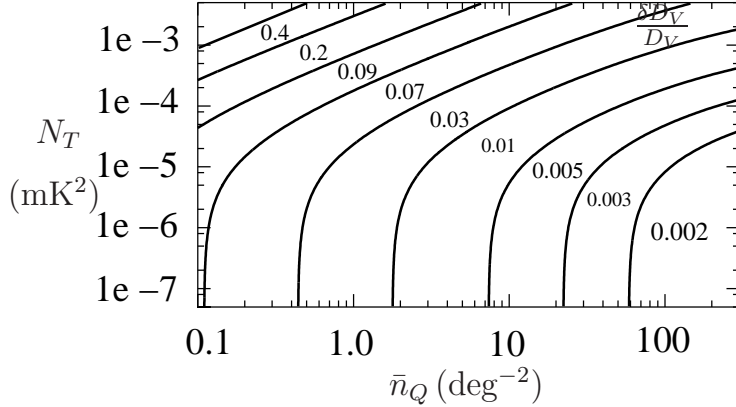


Figure 1. Contours of fractional errors in D_V at $z = 2.5$.

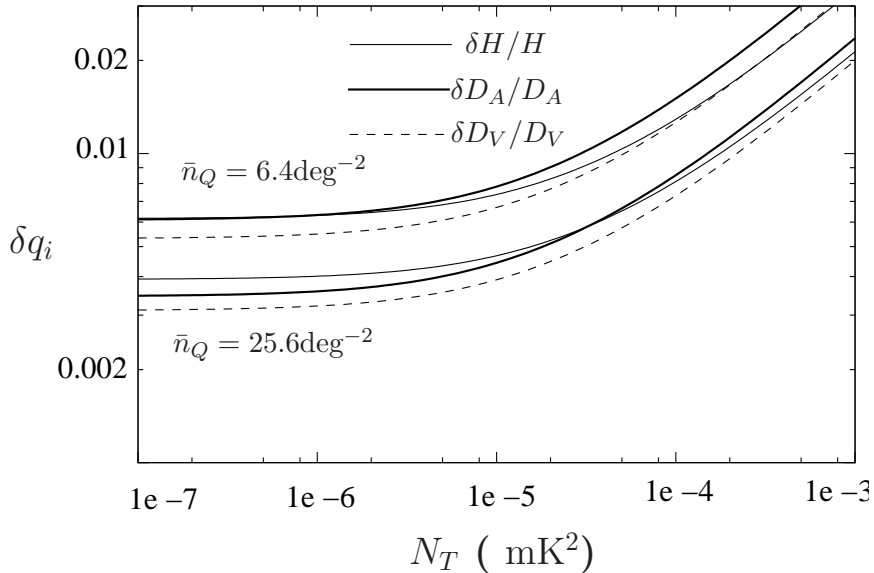


Figure 2. The variation of the fractional error in the parameters for a as a function of N_T , for fixed \bar{n}_Q corresponding to the BOSS and BIGBOSS like surveys. At large N_T we have $\delta q_i \propto \sqrt{N_T}$ asymptotically as shown by the broken line.

As outlined in Section 5, we have used a simple parametrization of the Lyman- α forest survey which very loosely matches some properties of the ongoing BOSS. We first apply our simple model to calculate the errors expected in the distance estimates from the auto-correlation signal for a BOSS-like survey. We use eq. (4.7) suitably modified for the Lyman- α forest auto-correlation. We find that our calculation predicts $\delta D_V/D_V = 2.0\%$ at $z = 2.5$ which is in close agreement with the detailed predictions [1]. In the subsequent analysis we consider $\delta D_V/D_V = 2.0\%$ as the fiducial error estimate for the auto-correlation and investigate if it is possible to improve this accuracy using the cross-correlation.

The sensitivity of the redshifted 21-cm observation is quantified by a single

parameter N_T . Figure 2 shows how the relative error in the distance estimates from the cross-correlation signal varies with N_T . We find that the errors scale as $\sqrt{N_T}$ for $N_T \geq 10^{-4} \text{mK}^2$. It is possible to achieve the fiducial value $\delta D_V/D_V = 2.0\%$ from the cross-correlation at $N_T = 2.9 \times 10^{-4} \text{mK}^2$. The error varies slower than $\sqrt{N_T}$ in the range $N_T = 10^{-4} \text{mK}^2$ to $N_T = 10^{-5} \text{mK}^2$. We have $(\delta D_V/D_V, \delta D_A/D_A, \delta H/H) = (1.3, 1.5, 1.3)\%$ and $(0.67, 0.78, 0.74)\%$ at $N_T = 10^{-4} \text{mK}^2$ and at $N_T = 10^{-5} \text{mK}^2$ respectively. The errors do not significantly go down much further for $N_T < 10^{-5} \text{mK}^2$, and we have $(0.55, 0.63, 0.63)\%$ at $N_T = 10^{-6} \text{mK}^2$. We see that it is possible to significantly increase the sensitivity relative to the BOSS Ly- α auto-correlation by considering the cross-correlation with redshifted 21-cm observations.

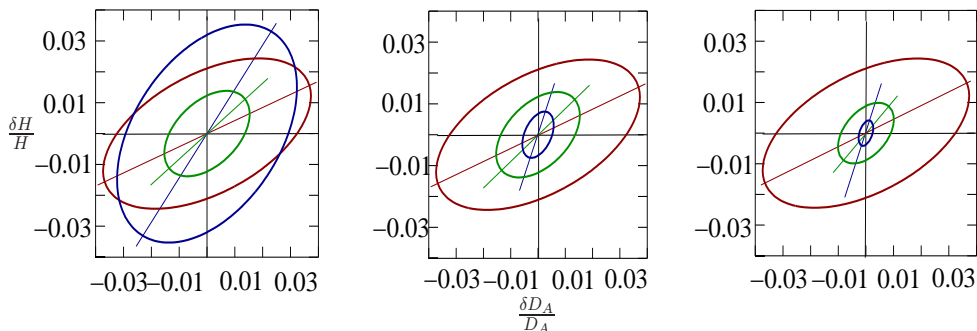


Figure 3. This shows $1 - \sigma$ contours for the BOSS Lyman- α forest auto-correlation (red), the redshifted 21-cm auto-correlation (blue) and the cross-correlation (green). The three panels consider $N_T = 10^{-4}, 10^{-5}$ and 10^{-6}mK^2 respectively (left to right).

Figure 3 shows a comparison of the relative errors in D_A and H for the three different estimates that can be obtained from the BOSS Lyman- α forest data and 21-cm observations, namely the respective auto-correlations and the cross-correlation. Note that each of the three estimates has a different sensitivity to the radial and transverse BAO signal, whereby the respective $1 - \sigma$ ellipses are differently oriented. The relatively large value of $\beta_{\mathcal{F}}$ for the Lyman- α forest make it more sensitive to the radial clustering. In contrast, the 21-cm is more sensitive to the transverse signal whereas the cross-correlation is oriented between the two auto-correlations. We find that it is possible to significantly increase the sensitivity relative to the BOSS Lyman- α forest auto-correlation by considering the cross-correlation with 21-cm observations. Note that it is particularly advantageous to use the cross-correlation in a situation where the two auto-correlations have comparable sensitivities ($N_T = 10^{-4} \text{mK}^2$ in this case). In such a situation we see that the cross-correlation provides more sensitive distance estimates compared to both the individual auto-correlation.

We now discuss the configuration of the radio-interferometric array and the observation time that will be required. It is necessary to balance the number of antennas N_{ann} and the total observing time T_{obs} which is divided over 25 pointings *ie.* $\Delta t = T_{obs}/25$ in eq. (5.1). An array with $N_{ann} = 2,000$ antennas will achieve $N_T = 3.1 \times 10^{-5} \text{mK}^2$ with 2 years of observation. With such an observation the cross-correlation will yield distance estimates with

$(\delta D_V/D_V, \delta D_A/D_A, \delta H/H) = (1.2, 1.4, 1.3) \%$ which is a 1.7 fold increase in the sensitivity relative to the BOSS Lyman- α forest auto-correlation. It is necessary to increase the number of antennas for a significant improvement beyond this. Considering an array with $N_{ann} = 4,000$ antennas, it will be possible to achieve $N_T = 3.9 \times 10^{-6} \text{mK}^2$ with 4 years of observation. This will yield distance estimates with $(\delta D_V/D_V, \delta D_A/D_A, \delta H/H) = (0.64, 0.74, 0.71) \%$ which is a 2.7 fold increase in the sensitivity relative to the BOSS Lyman- α forest auto-correlation. Finally, we find that the sensitivity of the cross-correlation with the BOSS Lyman- α forest does not increase beyond $(\delta D_V/D_V, \delta D_A/D_A, \delta H/H) = (0.53, 0.61, 0.62) \%$ irrespective of the number of antennas or the total observing time.

The BIGBOSS [53] has been conceived as the successor to BOSS. BIGBOSS may achieve a quasar density of $\sim 64 \text{deg}^{-2}$ which corresponds to $\bar{n}_Q = 25.6 \text{deg}^{-2}$. Our simple parametrization of the Lyman- α forest predicts $\delta D_V/D_V = 0.66 \%$ for the auto-correlation signal assuming $5 - \sigma$ SNR for all the spectra. This implies that the sensitivity of the auto-correlation signal increase by a factor of ~ 3 if the QSO number density is increased from $\bar{n}_Q = 6.4 \text{deg}^{-2}$ to $\bar{n}_Q = 25.6 \text{deg}^{-2}$. Considering the cross-correlation signal, we have, for $N_T = 1.0 \times 10^{-5} \text{mK}^2$, $(\delta D_V/D_V, \delta D_A/D_A, \delta H/H) = (0.39, 0.44, 0.47) \%$. We find that there is a ~ 1.7 fold increase in the sensitivity of the cross-correlation signal if we consider BIGBOSS instead of BOSS. This increase in sensitivity is approximately independent of the value of N_T .

In conclusion, our calculation indicates that it is possible to significantly increase the accuracy of the distance estimates by considering the cross-correlation signal. However, more detailed and realistic modelling of the Lyman- α data and the 21-cm observations are needed. We expect the predictions of the present analysis to serve as a useful signpost which indicates the direction for future work.

7 Acknowledgement

TGS would like to acknowledge Centre For Theoretical Studies, IIT Kharagpur for using its various facilities. TGS would also like to thank Tirthankar Roy Choudhury for useful discussions and help.

References

- [1] K. S. Dawson, D. J. Schlegel, C. P. Ahn, S. F. Anderson, É. Aubourg, S. Bailey, R. H. Barkhouser, J. E. Bautista, A. Beifiori, A. A. Berlind, V. Bhardwaj, and D. e. a. Bizyaev, *The Baryon Oscillation Spectroscopic Survey of SDSS-III*, *AJ* **145** (January, 2013) 10, [[arXiv:1208.0022](#)].
- [2] S. R. Furlanetto, S. P. Oh, and F. H. Briggs, *Cosmology at low frequencies: The 21 cm transition and the high-redshift Universe*, *Physics Report* **433** (October, 2006) 181–301, [[astro-ph/](#)].
- [3] M. F. Morales and J. S. B. Wyithe, *Reionization and Cosmology with 21 cm Fluctuations*, *ArXiv e-prints* (October, 2009) [[arXiv:0910.3010](#)].

- [4] D. H. Weinberg, S. Burles, R. A. C. Croft, R. Dave', G. Gomez, L. Hernquist, N. Katz, D. Kirkman, S. Liu, J. Miralda-Escude', M. Pettini, J. Phillips, D. Tytler, and J. Wright, *Cosmology with the Lyman-alpha Forest*, *ArXiv Astrophysics e-prints* (October, 1998) [[astro-ph/](#)].
- [5] R. Mandelbaum, P. McDonald, U. Seljak, and R. Cen, *Precision cosmology from the Lyman α forest: power spectrum and bispectrum*, *MNRAS* **344** (September, 2003) 776–788, [[astro-ph/](#)].
- [6] T. Guha Sarkar, S. Bharadwaj, T. R. Choudhury, and K. K. Datta, *Cross-correlation of the H I 21-cm signal and Ly α forest: a probe of cosmology*, *MNRAS* **410** (January, 2011) 1130–1134, [[arXiv:1002.1368](#)].
- [7] J. X. Prochaska, S. Herbert-Fort, and A. M. Wolfe, *The SDSS Damped Ly α Survey: Data Release 3*, *ApJ* **635** (December, 2005) 123–142, [[astro-ph/](#)].
- [8] S. Bharadwaj, B. B. Nath, and S. K. Sethi, *Using HI to Probe Large Scale Structures at $z \sim 3$* , *Journal of Astrophysics and Astronomy* **22** (March, 2001) 21–32, [[astro-ph/](#)].
- [9] R. A. C. Croft, D. H. Weinberg, N. Katz, and L. Hernquist, *Recovery of the Power Spectrum of Mass Fluctuations from Observations of the Ly alpha Forest*, *ApJ* **495** (March, 1998) 44–65, [[astro-ph/](#)].
- [10] S. Bharadwaj and S. K. Sethi, *HI Fluctuations at Large Redshifts: I Visibility correlation*, *Journal of Astrophysics and Astronomy* **22** (December, 2001) 293–307, [[astro-ph/](#)].
- [11] M. McQuinn and M. White, *On estimating Ly α forest correlations between multiple sightlines*, *MNRAS* **415** (August, 2011) 2257–2269, [[arXiv:1102.1752](#)].
- [12] A. Ghosh, S. Bharadwaj, S. S. Ali, and J. Chengalur, *GMRT Observation Towards Detecting the Post-reionization 21-cm Signal*, *Submitted to MNRAS* (2010).
- [13] A. Ghosh, S. Bharadwaj, S. Saiyad Ali, and J. N. Chengalur, *Improved foreground removal in GMRT 610 MHz observations towards redshifted 21-cm tomography*, *ArXiv e-prints* (August, 2011) [[arXiv:1108.3707](#)].
- [14] P. J. E. Peebles and J. T. Yu, *Primeval Adiabatic Perturbation in an Expanding Universe*, *ApJ* **162** (December, 1970) 815–825.
- [15] E. Komatsu, J. Dunkley, and M. R. e. a. Nolte, *Five-Year Wilkinson Microwave Anisotropy Probe Observations: Cosmological Interpretation*, *Astrophysical Journal Supplement* **180** (February, 2009) 330–376, [[arXiv:0803.0547](#)].
- [16] H. Seo and D. J. Eisenstein, *Probing Dark Energy with Baryonic Acoustic Oscillations from Future Large Galaxy Redshift Surveys*, *ApJ* **598** (December, 2003) 720–740, [[astro-ph/](#)].
- [17] M. White, *Baryon oscillations*, *Astroparticle Physics* **24** (December, 2005) 334–344, [[astro-ph/](#)].
- [18] T. Chang, U. Pen, J. B. Peterson, and P. McDonald, *Baryon Acoustic Oscillation Intensity Mapping of Dark Energy*, *Physical Review Letters* **100** (March, 2008) 091303, [[arXiv:0709.3672](#)].
- [19] X. Mao and X. Wu, *Signatures of the Baryon Acoustic Oscillations on 21 cm Emission Background*, *Astrophysical Journal Letters* **673** (February, 2008) L107–L110, [[arXiv:0709.3871](#)].

- [20] K. W. Masui, P. McDonald, and U. Pen, *Near-term measurements with 21 cm intensity mapping: Neutral hydrogen fraction and BAO at $z < 2$* , *PRD* **81** (May, 2010) 103527, [[arXiv:1001.4811](#)].
- [21] L. Anderson, E. Aubourg, S. Bailey, D. Bizyaev, M. Blanton, A. S. Bolton, J. Brinkmann, J. R. Brownstein, A. Burden, A. J. Cuesta, L. A. N. da Costa, K. S. Dawson, R. de Putter, D. J. Eisenstein, J. E. Gunn, H. Guo, J.-C. Hamilton, P. Harding, S. Ho, K. Honscheid, E. Kazin, D. Kirkby, J.-P. Kneib, A. Labatie, C. Loomis, R. H. Lupton, E. Malanushenko, V. Malanushenko, R. Mandelbaum, M. Manera, C. Maraston, C. K. McBride, K. T. Mehta, O. Mena, F. Montesano, D. Muna, R. C. Nichol, S. E. Nuza, M. D. Olmstead, D. Oravetz, N. Padmanabhan, N. Palanque-Delabrouille, K. Pan, J. Parejko, I. Pâris, W. J. Percival, P. Petitjean, F. Prada, B. Reid, N. A. Roe, A. J. Ross, N. P. Ross, L. Samushia, A. G. Sánchez, D. J. Schlegel, D. P. Schneider, C. G. Scóccola, H.-J. Seo, E. S. Sheldon, A. Simmons, R. A. Skibba, M. A. Strauss, M. E. C. Swanson, D. Thomas, J. L. Tinker, R. Tojeiro, M. V. Magaña, L. Verde, C. Wagner, D. A. Wake, B. A. Weaver, D. H. Weinberg, M. White, X. Xu, C. Yèche, I. Zehavi, and G.-B. Zhao, *The clustering of galaxies in the SDSS-III Baryon Oscillation Spectroscopic Survey: baryon acoustic oscillations in the Data Release 9 spectroscopic galaxy sample*, *MNRAS* **427** (December, 2012) 3435–3467, [[arXiv:1203.6594](#)].
- [22] P. McDonald and D. J. Eisenstein, *Dark energy and curvature from a future baryonic acoustic oscillation survey using the Lyman- α forest*, *PRD* **76** (September, 2007) 063009–063015, [[astro-ph/](#)].
- [23] N. G. Busca, T. Delubac, J. Rich, S. Bailey, A. Font-Ribera, D. Kirkby, J.-M. Le Goff, M. M. Pieri, A. Slosar, É. Aubourg, J. E. Bautista, D. Bizyaev, M. Blomqvist, A. S. Bolton, J. Bovy, H. Brewington, A. Borde, J. Brinkmann, B. Carithers, R. A. C. Croft, K. S. Dawson, G. Ebelke, D. J. Eisenstein, J.-C. Hamilton, S. Ho, D. W. Hogg, K. Honscheid, K.-G. Lee, B. Lundgren, E. Malanushenko, V. Malanushenko, D. Margala, C. Maraston, K. Mehta, J. Miralda-Escudé, A. D. Myers, R. C. Nichol, P. Noterdaeme, M. D. Olmstead, D. Oravetz, N. Palanque-Delabrouille, K. Pan, I. Pâris, W. J. Percival, P. Petitjean, N. A. Roe, E. Rollinde, N. P. Ross, G. Rossi, D. J. Schlegel, D. P. Schneider, A. Sheldon, E. S. Sheldon, A. Simmons, S. Snedden, J. L. Tinker, M. Viel, B. A. Weaver, D. H. Weinberg, M. White, C. Yèche, and D. G. York, *Baryon acoustic oscillations in the Ly α forest of BOSS quasars*, *Astronomy and Astrophysics* **552** (April, 2013) A96, [[arXiv:1211.2616](#)].
- [24] A. Slosar, V. Iršič, D. Kirkby, S. Bailey, N. G. Busca, T. Delubac, J. Rich, É. Aubourg, J. E. Bautista, V. Bhardwaj, M. Blomqvist, A. S. Bolton, J. Bovy, J. Brownstein, B. Carithers, R. A. C. Croft, K. S. Dawson, A. Font-Ribera, J.-M. Le Goff, S. Ho, K. Honscheid, K.-G. Lee, D. Margala, P. McDonald, B. Medolin, J. Miralda-Escudé, A. D. Myers, R. C. Nichol, P. Noterdaeme, N. Palanque-Delabrouille, I. Pâris, P. Petitjean, M. M. Pieri, Y. Piškur, N. A. Roe, N. P. Ross, G. Rossi, D. J. Schlegel, D. P. Schneider, N. Suzuki, E. S. Sheldon, U. Seljak, M. Viel, D. H. Weinberg, and C. Yèche, *Measurement of baryon acoustic oscillations in the Lyman- α forest fluctuations in BOSS data release 9*, *JCAP* **4** (April, 2013) 26, [[arXiv:1301.3459](#)].
- [25] T. Guha Sarkar and S. Bharadwaj, *The Imprint of the Baryon Acoustic Oscillations (BAO) in the Cross-correlation of the Redshifted HI 21-cm Signal and the Ly-alpha Forest*, *ArXiv e-prints* (December, 2011) [[arXiv:1112.0745](#)].
- [26] J. E. Gunn and B. A. Peterson, *On the Density of Neutral Hydrogen in*

- Intergalactic Space.*, *ApJ* **142** (November, 1965) 1633–1641.
- [27] H. Bi and A. F. Davidsen, *Evolution of Structure in the Intergalactic Medium and the Nature of the Ly α Forest*, *ApJ* **479** (April, 1997) 523–532, [[astro-ph/](#)].
- [28] R. A. C. Croft, D. H. Weinberg, M. Pettini, L. Hernquist, and N. Katz, *The Power Spectrum of Mass Fluctuations Measured from the LY α Forest at Redshift $Z=2.5$* , *ApJ* **520** (July, 1999) 1–23, [[astro-ph/](#)].
- [29] T. Kim, J. S. Bolton, M. Viel, M. G. Haehnelt, and R. F. Carswell, *An improved measurement of the flux distribution of the Ly α forest in QSO absorption spectra: the effect of continuum fitting, metal contamination and noise properties*, *MNRAS* **382** (December, 2007) 1657–1674, [[arXiv:0711.1862](#)].
- [30] P. McDonald, J. Miralda-Escudé, M. Rauch, W. L. W. Sargent, T. A. Barlow, and R. Cen, *A Measurement of the Temperature-Density Relation in the Intergalactic Medium Using a New Ly α Absorption-Line Fitting Method*, *ApJ* **562** (November, 2001) 52–75, [[astro-ph/](#)].
- [31] T. R. Choudhury, T. Padmanabhan, and R. Srianand, *Semi-analytic approach to understanding the distribution of neutral hydrogen in the Universe*, *MNRAS* **322** (April, 2001) 561–575, [[astro-ph/](#)].
- [32] M. Viel, S. Matarrese, H. J. Mo, M. G. Haehnelt, and T. Theuns, *Probing the intergalactic medium with the Ly α forest along multiple lines of sight to distant QSOs*, *MNRAS* **329** (February, 2002) 848–862, [[astro-ph/](#)].
- [33] F. Saitta, V. D’Odorico, M. Bruscoli, S. Cristiani, P. Monaco, and M. Viel, *Tracing the gas at redshift 1.7-3.5 with the Ly α forest: the FLO approach*, *MNRAS* **385** (March, 2008) 519–530, [[arXiv:0712.2452](#)].
- [34] A. Slosar, S. Ho, M. White, and T. Louis, *The acoustic peak in the Lyman alpha forest*, *Journal of Cosmology and Astro-Particle Physics* **10** (October, 2009) 19–24, [[arXiv:0906.2414](#)].
- [35] L. Fang, H. Bi, S. Xiang, and G. Boerner, *Linear evolution of cosmic baryonic medium on large scales*, *ApJ* **413** (August, 1993) 477–485.
- [36] S. Wyithe and A. Loeb, *Fluctuations in 21cm Emission After Reionization*, *ArXiv e-prints* (August, 2007) [[arXiv:0708.3392](#)].
- [37] J. S. B. Wyithe and A. Loeb, *The 21-cm power spectrum after reionization*, *MNRAS* **397** (August, 2009) 1926–1934.
- [38] F. Marin, N. Y. Gnedin, H. Seo, and A. Vallinotto, *Modeling The Large Scale Bias of Neutral Hydrogen*, *ArXiv e-prints* (November, 2009) [[arXiv:0911.0041](#)].
- [39] J. S. Bagla, N. Khandai, and K. K. Datta, *HI as a Probe of the Large Scale Structure in the Post-Reionization Universe*, *ArXiv e-prints* (August, 2009) [[arXiv:0908.3796](#)].
- [40] T. Guha Sarkar, S. Mitra, S. Majumdar, and T. R. Choudhury, *Constraining large scale HI bias using redshifted 21-cm signal from the post-reionization epoch*, *ArXiv e-prints* (September, 2011) [[arXiv:1109.5552](#)].
- [41] P. McDonald, *Toward a Measurement of the Cosmological Geometry at $z \sim 2$: Predicting Ly- α Forest Correlation in Three Dimensions and the Potential of Future Data Sets*, *ApJ* **585** (March, 2003) 34–51, [[astro-ph/](#)].
- [42] P. McDonald, U. Seljak, S. Burles, and D. J. e. a. Schlegel, *The Ly α Forest*

- Power Spectrum from the Sloan Digital Sky Survey*, *ApJS* **163** (March, 2006) 80–109, [[astro-ph/](#)].
- [43] K. K. Datta, T. R. Choudhury, and S. Bharadwaj, *The multifrequency angular power spectrum of the epoch of reionization 21-cm signal*, *MNRAS* **378** (June, 2007) 119–128, [[astro-ph/](#)].
- [44] A. D. Myers, R. J. Brunner, G. T. Richards, R. C. Nichol, D. P. Schneider, and N. A. Bahcall, *Clustering Analyses of 300,000 Photometrically Classified Quasars. II. The Excess on Very Small Scales*, *ApJ* **658** (March, 2007) 99–106, [[astro-ph/](#)].
- [45] G. D. Becker, W. L. W. Sargent, and M. Rauch, *Large-Scale Correlations in the Ly α Forest at $z = 3-4$* , *ApJ* **613** (September, 2004) 61–76, [[astro-ph/](#)].
- [46] F. Coppolani, P. Petitjean, F. Stoehr, E. Rollinde, C. Pichon, S. Colombi, M. G. Haehnelt, B. Carswell, and R. Teyssier, *Transverse and longitudinal correlation functions in the intergalactic medium from 32 close pairs of high-redshift quasars*, *MNRAS* **370** (August, 2006) 1804–1816, [[astro-ph/](#)].
- [47] V. D’Odorico, M. Viel, F. Saitta, S. Cristiani, S. Bianchi, B. Boyle, S. Lopez, J. Maza, and P. Outram, *Tomography of the intergalactic medium with Ly α forests in close QSO pairs*, *MNRAS* **372** (November, 2006) 1333–1344, [[astro-ph/](#)].
- [48] L. Jiang, X. Fan, and R. J. e. Cool, *A Spectroscopic Survey of Faint Quasars in the SDSS Deep Stripe. I. Preliminary Results from the Co-added Catalog*, *Astrophysical Journal* **131** (June, 2006) 2788–2800, [[astro-ph/](#)].
- [49] J. N. Chengalur, Y. Gupta, and K. S. Dwarkanath, *“Low Frequency Radio Astronomy”*. NCRA-TIFR, India, 2007.
- [50] H.-J. Seo and D. J. Eisenstein, *Improved Forecasts for the Baryon Acoustic Oscillations and Cosmological Distance Scale*, *ApJ* **665** (August, 2007) 14–24, [[astro-ph/](#)].
- [51] D. J. Eisenstein, I. Zehavi, D. W. Hogg, R. Scoccimarro, M. R. Blanton, R. C. Nichol, R. Scranton, and et al., *Detection of the Baryon Acoustic Peak in the Large-Scale Correlation Function of SDSS Luminous Red Galaxies*, *ApJ* **633** (November, 2005) 560–574, [[astro-ph/](#)].
- [52] D. P. Schneider, P. B. Hall, G. T. Richards, and D. E. e. Vanden Berk, *The Sloan Digital Sky Survey Quasar Catalog. III. Third Data Release*, *Astrophysical Journal* **130** (August, 2005) 367–380, [[astro-ph/](#)].
- [53] D. J. Schlegel, C. Bebek, H. Heetderks, S. Ho, and M. Lampton, *BigBOSS: The Ground-Based Stage IV Dark Energy Experiment*, *ArXiv e-prints* (April, 2009) [[arXiv:0904.0468](#)].